The parameters for the 256 × 256 image of tree bark texture in Fig. 5 are given in Table II.

REFERENCES

[1] D. A. Bader, J. JáJá, and R. Chellappa, "Scalable data parallel algorithms for texture synthesis and compression using Gibbs random fields," UMIACS and Elec. Eng., Univ. of Maryland, College Park, MD, Tech. Rep. CS-TR-3123 and UMIACS-TR-93-80, Aug. 1993.

[2] J. E. Besag and P. A. P. Moran, "On the estimation and testing of spacial interaction in Gaussian lattice processes," *Biometrika*, vol. 62, pp. 555–562, 1975.

[3] R. Chellappa, "Two-dimensional discrete Gaussian Markov random field models for image processing," in *Progress in Pattern Recognition*, vol. 2, L. N. Kanal and A. Rosenfeld, Eds. New York: Elsevier, 1985, pp. 79–112.

[4] R. Chellappa and R. L. Kashyap, "Synthetic generation and estimation in random field models of images," in *Proc. IEEE Comp. Soc. Conf. Patt. Recog. Image Processing*, Dallas, TX, Aug. 1981, pp. 577–582.

[5] F. S. Cohen, "Markov random fields for image modeling and analysis," in *Modelling and Applications of Stochastic Processes*, U. Desai, Ed. Boston, MA: Kluwer, 1986, pp. 243–272, ch. 10.

[6] G. R. Cross and A. K. Jain, "Markov random field texture models," *IEEE Trans. Pattern. Anal. Machine Intell.*, vol. PAMI-5, pp. 25–39, Jan. 1983.

[7] R. C. Dubes and A. K. Jain, "Random field models in image analysis," *J. Applied Statist.*, vol. 16, pp. 131–164, 1989.

[8] S. Geman and D. Geman, "Stochastic relaxation, Gibbs distributions, and the Bayesian restoration of images," *IEEE Trans. Pattern Anal. Machine Intell.*, vol. PAMI-6, pp. 721–741, Nov. 1984.

[9] F. C. Jeng, J. W. Woods, and S. Rastogi, "Compound Gauss–Markov random fields for parallel image processing," in *Markov Random Fields: Theory and Application*, R. Chellappa and A. K. Jain, Eds. Boston, MA: Academic, 1993, chap. 2, pp. 11–38.

[10] R. L. Kashyap and R. Chellappa, "Estimation and choice of neighbors in spacial interaction models of images," *IEEE Trans. Inform. Theory*, vol. IT-29, pp. 60–72, Jan. 1983.

Linear Filtering of Images Based on Properties of Vision

V. Ralph Algazi, Gary E. Ford, and Hong Chen

***Abstract*— The design of linear image filters based on properties of human visual perception has been shown to require the minimization of criterion functions in both the spatial and frequency domains. In this correspondence, we extend this approach to continuous filters of infinite support. For lowpass filters, this leads to the concept of an ideal lowpass image filter that provides a response that is superior perceptually to that of the classical ideal lowpass filter.**

I. INTRODUCTION

THE use of hard cutoff (ideal) lowpass filters in the suppression of additive image noise is known to produce ripples in the response to sharp edges. For high contrast edges, human visual perception fairly simply determines acceptable filter behavior. Ripples in the filter response are visually masked by the edge, so that the contrast sensitivity of the visual system decreases at sharp transitions in image intensity and increases somewhat exponentially as a function of the spatial distance from the transition.

Algorithmic procedures using properties of human vision have been described for over 20 years [1]. The development of adaptive methods of image enhancement and restoration, based on the use of a masking function, measure spatial detail to determine visual masking [2], [3]. In active regions of the image, visual masking is high, relative noise visibility is low, and the filter applied is allowed to pass more noise until the subjective visibility is equal to that in flat areas.

Whether the filter is adaptive or not, the design of the linear filter to be applied is a critical issue. Hentea and Algazi [4] have demonstrated that the first perceptible image distortions due to linear filtering occur at the major edges and thus, worst case design for visual appearance should be based on edge response. They developed a filter design approach based on the minimization of a weighted sum of squared-error criterion functions in both the spatial and frequency domains. In the spatial domain, the weighting is by a visibility function, representing the relative visibility of spatial details as a monotonically increasing function of the distance from an edge. This visibility function, determined experimentally from the visibility of a short line positioned parallel to an edge, was also found experimentally to predict satisfactorily the visibility of ripples due to linear filters [4].

In the following, we extend the work of Hentea and Algazi by considering the design and properties of one-dimensional continuous filters of infinite support (two-dimensional filters are generated by 1 D to 2 D transformations). We obtain a new formal result on the lowpass filter of infinite support that is optimal for images. It establishes the limiting performance that digital filters of finite complexity can only approximate.

II. DESIGN OF ONE-DIMENSIONAL FILTERS FOR IMAGES

The basic tradeoff in the design approach of Algazi and Hentea [4] is maintaining image quality while reducing unwanted artifacts or noise. The image quality is measured by spatial domain criterion function for the visibility of ripples in the vicinity of edges

$$I_1 = \int_{-\infty}^{\infty} w_1^2(x)[\hat{u}(x) - u(x)]^2\,dx \tag{1}$$

where $u(x)$ is a unit step input producing the filter response $\hat{u}(x) = u(x) * h(x)$, where $h(x)$ is the point spread function of the filter, $*$ denotes convolution and $w_1(x)$ is a spatial weighting function, chosen to be the visibility function

$$w_1(x) = 1 - a^{|x|}. \tag{2}$$

The frequency domain criterion function for the reduction of unwanted artifacts and noise is

$$I_2 = \int_{-\infty}^{\infty} W_2^2(f)|H(f) - H_d(f)|^2\,df \tag{3}$$

where $H_d(f)$ is the desired filter frequency response and $W_2(f)$ is the frequency-domain weighting function. Hentea and Algazi minimized I_1 under a constraint on I_2, but we now minimize the equivalent criterion $J(\alpha) = \alpha I_1 + (1 - \alpha)I_2$ where α controls the relative weights of the two criteria, with $0 \le \alpha \le 1$.

To develop the optimality condition, (1) is expressed in the frequency domain using Parseval's relation, the transform of a zero-mean step is used, and calculus of variations is applied to the criterion

Manuscript received November 5, 1993; revised December 21, 1994. This work was supported by the University of California MICRO Program, Grass Valley Group, Pacific Bell, Lockheed, and Hewlett Packard. The associate editor coordinating the review of this paper and approving it for publication was Prof. Nikolas P. Galatsanos.

The authors are with the CIPIC, Center for Image Processing and Integrated Computing, University of California, Davis, Davis, CA 95616 USA.

IEEE Log Number 9413843.

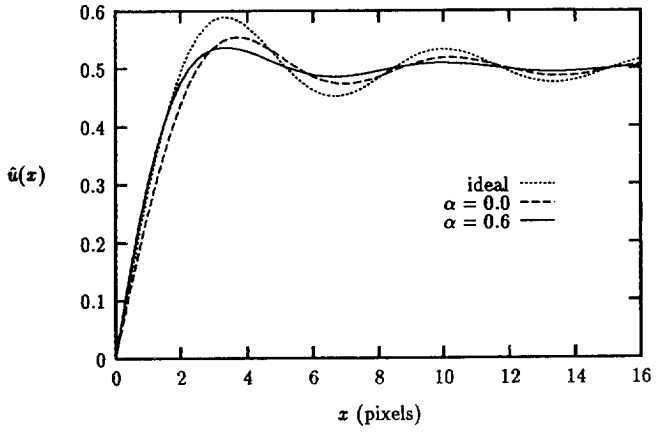

Fig. 1. Comparison of filter step responses.

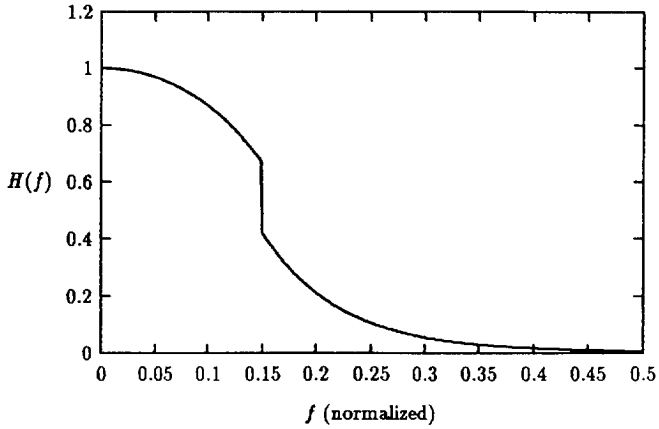

Fig. 2. Lowpass image filter frequency response for $\alpha = 0.60$.

J, resulting in the condition

$$\alpha\left\{W_1(f) * \left[\frac{H(f)-1}{j2\pi f}\right]\right\} = (1-\alpha)j2\pi f W_2^2(f)[H(f) - H_d(f)]. \quad (4)$$

Substituting the spatial weighting function of (2), with Fourier transform

$$W_1(f) = \delta(f) - \frac{2b}{b^2 + (2\pi f)^2} \quad (5)$$

with $b = -\ln \alpha$, (4) becomes

$$H(f) = \frac{1}{\beta(2\pi f)^2 W_2^2(f)}\left((2\pi f)^2 W_2^2(f) H_d(f) + \left\{\frac{b^2}{b^2 + (2\pi f)^2} + j2\pi f\left[\frac{2b}{b^2 + (2\pi f)^2} * \frac{H(f)}{j2\pi f}\right]\right\}\right) \quad (6)$$

where $\beta = (1-\alpha)/\alpha$. This is a linear Fredholm integral equation of the second kind and a discussion of the solution of this equation in terms of eigenfunctions of an equation of similar form arising from a related approach to filter design is given in [5]. That approach is practically useful only if the solution to the homogeneous equation related to (6) is known in closed form or tabulated, which is not the case for our problem. Thus, in the design examples discussed below, we apply a series solution.

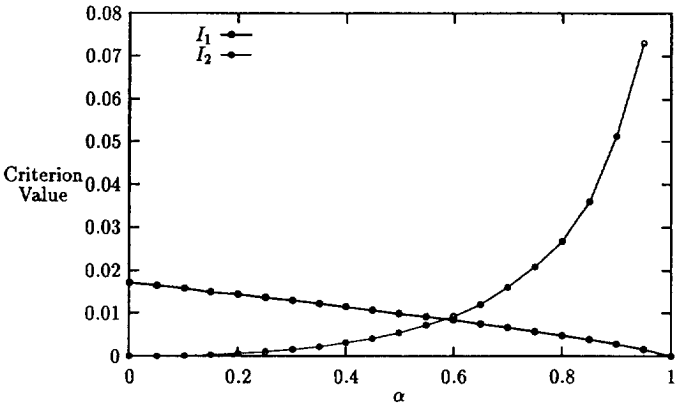

Fig. 3. Design criteria I_1 and I_2 as a function of α.

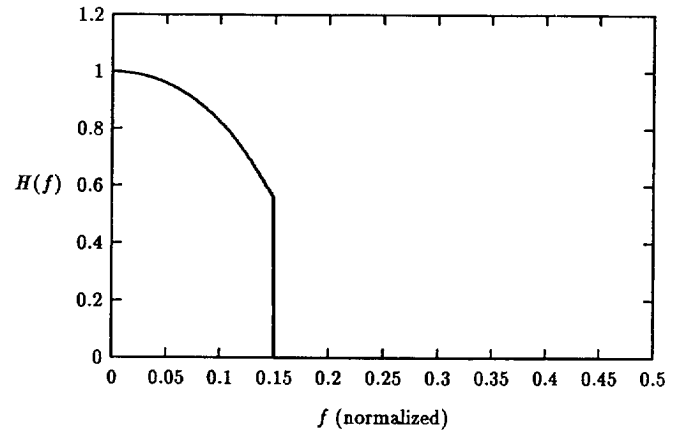

Fig. 4. Frequency response for ideal lowpass image filter $\alpha = 0$.

III. Lowpass Image Filter Design

For a lowpass image filter, the desired frequency response is

$$H_d(f) = \begin{cases} 1, & |f| \le f_c \\ 0, & |f| > f_c \end{cases} \quad (7)$$

where f_c is the filter cutoff frequency. We choose $W_2(f)$ to weight the stopband response only

$$W_2(f) = \begin{cases} 0 & |f| \le f_c \\ 1 & |f| > f_c \end{cases}. \quad (8)$$

The conditions of (7) and (8) are applied to the integral equation (6). The resulting equation is solved with the Neumann series solution, an iterative approach in which an approximation to $H(f)$ used in the convolution integral on the right-hand side of (6) generates the next approximate solution. Let the kth approximation to $H(f)$ be $\hat{H}_k(f)$, then the $(k+1)$th approximation is

$$\hat{H}_{k+1}(f) = H_a(f)\left\{\frac{b^2}{b^2 + (2\pi f)^2} + j2\pi f\left[\frac{2b}{b^2 + (2\pi f)^2} * \frac{\hat{H}_k(f)}{j2\pi f}\right]\right\} \quad (9)$$

where

$$H_a(f) = \begin{cases} 1 & |f| \le f_c \\ \dfrac{1}{1 + \beta(2\pi f)^2} & |f| > f_c \end{cases}. \quad (10)$$

The initial condition for the iterative solution is $\hat{H}_0(f) = H_a(f)$. In the examples considered, we observed that the solutions converged

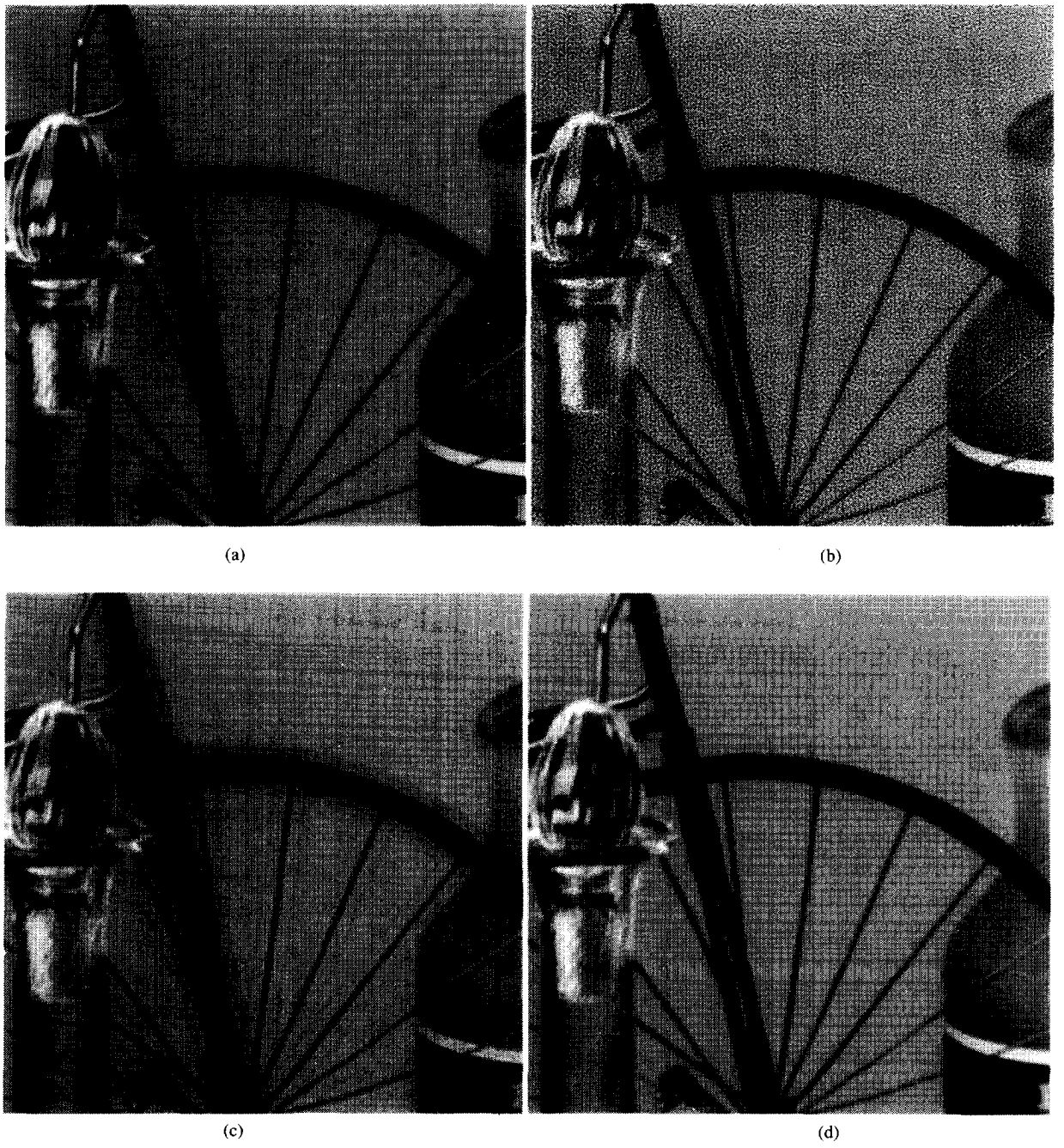

Fig. 5. Lowpass filtering. (a) Original image; (b) noisy image; (c) noisy image processed with an equiripple low-pass filter; and (d) noisy image processed with a lowpass image filter, $\alpha = 0.6$.

to an accuracy of three decimal places in only eight iterations, convergence was not strongly affected by the initial condition, and there was no indication that the solution was not unique. A discussion of convergence for a series solution to a similar integral equation is given in [5].

As an example, consider the design of a lowpass filter with cutoff frequency $f_c = 0.15$ (normalized) and $\alpha = 0.6$. Normalizing the viewing distance to six times the image height, the resulting angular increment is 1.116 minutes of arc per pixel and the appropriate value for a in $w_1(x)$ is 0.72 ($b = 0.33$) [4]. The ripples in the step response of the resulting figure, shown in Fig. 1, are strongly suppressed. The frequency response of filter is shown in Fig. 2.

The plot showing the tradeoff between I_1 and I_2 as a function of α in Fig. 3 can be used to choose α to meet specifications on I_1 or I_2. Note the large decrease in the frequency domain rejection that is required for a small improvement in spatial domain response.

Of independent interest is the ideally bandlimited lowpass image filter, which results from setting $\alpha \to 0$ or $\beta \to \infty$. The filter design in this case is equivalent to minimizing spatial domain criterion I_1 under the constraint that the stopband energy of I_2 be zero.

The form of (9) remains the same, but $H_u(f)$ [and the initial condition $\hat{H}_0(f)$] becomes the frequency response of the classical ideal lowpass filter

$$H_u(f) = \begin{cases} 1 & |f| \le f_c \\ 0 & |f| > f_c \end{cases}. \tag{11}$$

The step response of an example filter with cutoff frequency $f_c = 0.15$ (normalized) and $a = 0.72$, shown in Fig. 1, has a ripple

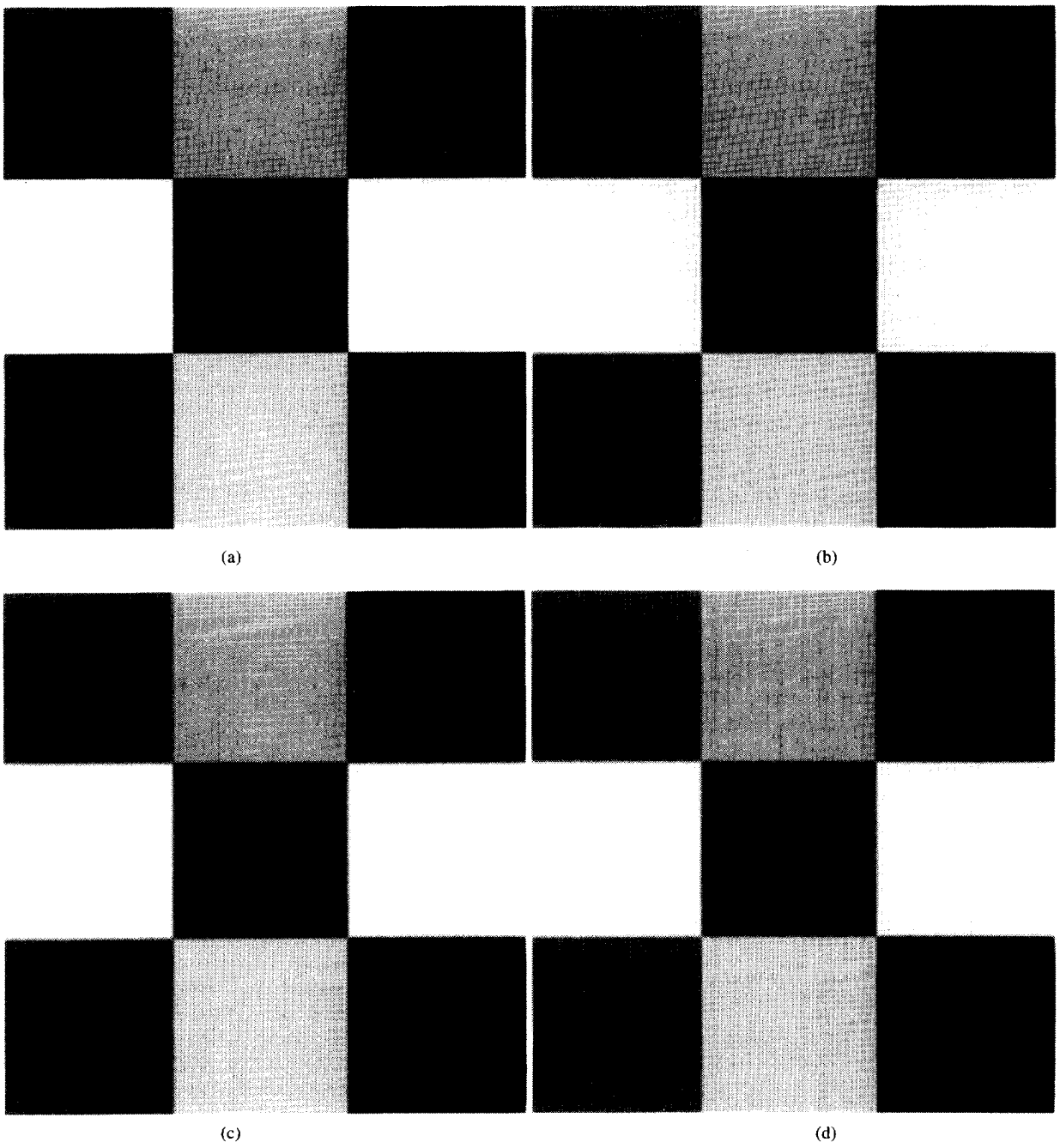

Fig. 6. Image filtering by lowpass filters. (a) Original image; (b) filtered with classical ideal lowpass filter; (c) filtered with ideal lowpass image filter, $\alpha = 0$; and (d) filtered with lowpass image filter, $\alpha = 0.6$.

response that is better than that of the classical ideal lowpass filter. The spatial error integral I_1 for the ideal image lowpass filter is 45% less than that for the classical ideal lowpass filter. The filter frequency response for this example is shown in Fig. 4.

IV. Lowpass Filter Examples

To illustrate the properties of the lowpass image filters discussed in the section above, we consider two-dimensional FIR approximations of the design examples and compare performance with that of an equiripple filter on a noisy image. To ensure ease of comparison of the halftone reproductions in a journal publication, a test image with substantial distortion was chosen. The results clearly extend to images of lower contrast and smaller distortions. High frequency noise was added to the original image of Fig. 5(a) by highpass filtering noise with a uniform distribution, producing the noisy image shown in Fig. 5(b), having peak signal-to-noise ratio (PSNR) of 8.22 dB.

The noisy image was filtered by an equiripple lowpass filter that approximates an ideal lowpass filter, and a lowpass image filter design with our approach, each having the same maximum deviation in the stopband and cutoff frequency $f_c = 0.15$ (normalized frequency). The lowpass image filter is based on the 1-D design with $\alpha = 0.6$, having frequency response shown in Fig. 2. The applied filters are 2-D circularly symmetric, obtained from 1-D filters by McClellan's transformation [6]. The equiripple filter response in Fig. 5(c) shows strong ripple responses at major transitions and it produces a PSNR of 25.5 dB. The lowpass image filter response in Fig. 5(d) has

suppressed the ripples and produced an improved PSNR of 32.3 dB. Thus, the lowpass image filter is superior perceptually and it provides better noise reduction.

The ripple responses of the lowpass filters are compared in the checkerboard images of Fig. 6. Fig. 6(b)–(d) show the responses of filters having a cutoff frequency $f_c = 0.15$ (normalized frequency). The response of a classical ideal lowpass filter is shown in Fig. 6(b), showing very strong ripple response. The response of the ideal lowpass image filter of Section III, with $\alpha = 0$ and having the frequency response of Fig. 4 is shown in Fig. 6(c), where the ripples have decreased substantially. Finally, in the response to the lowpass image filter from Section III, with frequency response shown in Fig. 2 for $\alpha = 0.6$, the ripples are difficult to perceive.

V. Discussion and Conclusions

We have reconsidered a method for the design of linear filters for image processing based on properties of the human visual system, which involves the minimization of criterion functions in both the spatial and frequency domains. We have extended this work by obtaining new theoretical results by considering continuous filters of infinite support.

An important limiting result for an ideal lowpass image filter having infinite support has been obtained. This ideal lowpass image filter is greatly superior perceptually to the classical lowpass filter and provides a design target for the important problems of image sampling and interpolation. We have found that interpolation filters designed with this approach provide better results than bicubic filters that approximate classical ideal lowpass filters [7].

References

[1] B. R. Hunt, "Digital image processing," *Proc. IEEE,* vol. PROC-63, pp. 693–708, 1975.

[2] G. L. Anderson and A. N. Netravali, "Image restoration based on a subjective criterion," *IEEE Trans. Syst., Man, Cybern.,* vol. SMC-6, no. 12, pp. 845–853, 1976.

[3] A. Katsaggelos, "Iterative image restoration algorithms," *Opt. Eng.,* vol. 28, pp. 735–748, 1989.

[4] T. A. Hentea and V. R. Algazi, "Perceptual models and the filtering of high-contrast achromatic images," *IEEE Trans. Syst., Man, Cybern.,* vol. SMC-14, no. 2, pp. 230–246, 1984.

[5] V. R. Algazi and M. Suk, "On the frequency weighted least-square design of finite duration filters," *IEEE Trans. Circuits Syst.,* vol. 22, no. 12, pp. 943–953, 1975.

[6] J. H. McClellan, "The design of two-dimensional digital filters by transformations," in *Proc. 7th Annu. Princeton Conf. Inform. Sci. Syst.,* 1973, pp. 247–251.

[7] H. Chen and G. E. Ford, "An FIR image interpolation filter design method based on properties of human vision," in *Proc. IEEE Int. Conf. Image Processing,* 1994, vol. III, pp. 581–585.

On the Computational Model of a Kind of Deconvolution Problem

Zou Mou-yan and Rolf Unbehauen

***Abstract*—It is known that discretization of a continuous deconvolution problem can alleviate the ill-posedness of the problem. The currently used circulant matrix model, however, does not play such a role. Moreover, the approximation of deconvolution problems by circulant matrix model is rational only if the size of the kernel function is very small. In this correspondence, we propose an aperiodic model of deconvolution. For discrete and finite deconvolution problems the new model is an exact one. In the general case, the new model can lead to a nonsingular system of equations that has a lower condition number than the circulant one, and the related computations in the deconvolution can be done efficiently by means of the DFT technique, as in the case for circulant matrices. The rationality of the new model holds without regard to the size of the kernel and the image. The use of the aperiodic model is illustrated by gradient-based algorithms.**

I. Introduction

A kind of image restoration or, more generally, signal restoration by deconvolution will involve the solution of a Fredholm equation of the first kind

$$\int_{-\infty}^{\infty} h(\mu - \nu)x(\nu)d\nu = y(\mu) \tag{1}$$

where

- h convolution kernel
- x unknown object
- y observation.

In the 2-D case, the arguments μ and ν should be understood as vectors in the continuum $\mathcal{R}^2$. In usual cases, the equation is ill-posed in the sense that the result of the deconvolution is sensitive to perturbation of the observation and the kernel function. The ill-posedness of (1) may be explained by means of the Riemann–Lebesgue lemma [3, pp. 114–115]. From this lemma, (1) inevitably involves some parasitic solutions with very high frequencies. Since it is very difficult to have an "exact" solution, naturally, we can expect some *physically rational solution* of the problem. Tikhonov first treated this problem on a strict mathematical basis [1] by introducing the regularization theory and methods. Generally speaking, regularization encompasses a class of solution techniques that modify an ill-posed problem into a well-posed one by approximation so that a physically acceptable approximate solution can be obtained, and the solution is sufficiently stable from the computational viewpoint [2].

For digital processing, the observation y must be digitized, and the convolution equation must be replaced by a discrete convolution that can be put into the algebraic equation form

$$\boldsymbol{Bx} = \boldsymbol{y} \tag{2}$$

Manuscript received December 21, 1993; revised December 21, 1994. This work was supported by the German Research Association, Deutsche Forschungsgemeinschaft, Germany. The associate editor coordinating the review of this paper and approving it for publication was Prof. Xinhua Zhuang.

M.-Y. Zou is with the Lehrstuhl für Allgemeine und Theoretische Elektrotechnik, Universität Erlangen-Nürnberg, Erlangen, Germany, on leave from the Institute of Electronics, Academia Sinica, Beijing, China.

R. Unbehauen is with the with Lehrstuhl für Allgemeine und Theoretische Elektrotechnik, Universität Erlangen-Nürnberg, Erlangen, Germany.

IEEE Log Number 9413845.